The Compleat Gamma Pulse

Cye H. Waldman
cye@att.net

The gamma pulse is a model transient pulse that was designed for application to physical systems. It can be convolved with impulsive solutions in temporal or harmonic space to develop the transient response to an input pulse. It has many interesting mathematical properties as well, and can be used as a plane curve generator in the complex plane. In this brief note we discuss application to plane curves and physical pulses. Thus, without any further ado, we introduce the gamma pulse,

$$\begin{aligned} &\gamma(\tau;n) = \tau^n e^{-\tau} u(\tau) \\ &\int_0^\infty \gamma(\tau;n)\,d\tau = \Gamma(n+1) \end{aligned} \tag{1}$$

where u is the Heaviside function, the parameter τ can be likened to a (dimensionless) time, and the complex constant n is referred to as the pulse order. The pulse derives its name from the fact that it is the kernel of the well-known gamma function. Plane curves arise with complex n, whereas real, positive n lead to models of physical pulses.

Plane curves

We shall first describe some general properties of the gamma pulse and then give some specific examples of plane curves. The gamma pulse is related to the Cauchy pulse through the Fourier transform as follows:

$$\begin{aligned} &\mathscr{F}\{\psi(\tau;n)\} = 2\pi\, i^n \gamma(\varpi;n) \\ &\mathscr{F}\{\gamma(\tau;n)\} = i^n \psi^*(\varpi;n) \\ &\int_{-\infty}^{\infty} |\psi(\tau;n)|^2\, d\tau = 2\pi \int_0^\infty \gamma^2(\varpi;n)\,d\varpi \end{aligned} \tag{2}$$

where ϖ is the (dimensionless) frequency. The Cauchy pulse has been described previously (http://curvebank.calstatela.edu/waldman/waldman.htm) and is given by

$$\psi(\tau;n) = \frac{i^n\,\Gamma(n+1)}{(1-i\tau)^{n+1}} \tag{3}$$

The Cauchy pulse is amenable to the fractional calculus and the pulse order n can be literally anything: rational or irrational, real or complex. Mathematically, this carries over to the gamma pulse and allows us to explore plane curves in the complex plane. The gamma pulse itself is *not* amenable to the fractional calculus, but merely enjoys the freedom of exponentiation.

Fractional derivatives of the gamma pulse can be derived from the following equation from K.B. Oldham and J. Spanier, *The Fractional Calculus*, Dover, 1974,

$$\frac{d^q}{dx^q}\left(\frac{\exp(-1/x)}{x^{1-q}}\right)=\frac{\exp(-1/x)}{x^{1+q}} \tag{4}$$

Here we see the right-hand-side is equal to $\gamma(\tau;1+q)$ upon the transformation $\tau=1/x$. Therefore, we can derive the following fractional derivative for the gamma pulse,

$$\left[-\tau^2\frac{d}{d\tau}\right]^q\gamma(\tau;1-q)=\gamma(\tau;1+q) \tag{5}$$

We now turn our attention the gamma pulse as a plane curve generator. This requires that *n* is complex, of course. There are two curve types in the gamma pulse family; depending on whether *n* is purely imaginary or complex. When *n* is purely imaginary we find a type of spiral that is previously unknown to us. An example is shown in Figure 1 for *n* = 10*i*. Starting from the origin ($\tau=\infty$) the spiral opens up in the usual way, but instead of expanding ever outward it reaches a limit cycle at the unit circle with the concentric rings getting tighter as the limit cycle is approached. As *n* increases or decreases, so does the number of revolutions to reach the limit.

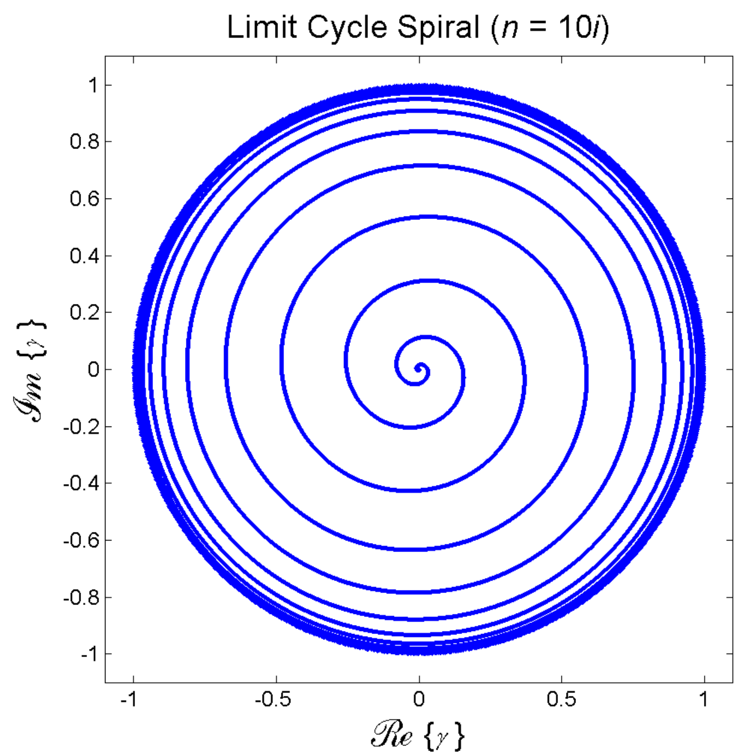

Figure 1: Limit cycle spiral (*n* = 10i).

The limit cycle is a reminder that any real positive number raised to an imaginary power lies on the unit circle, i.e., $x^{ai} = \cos(a\ln x) + i\sin(a\ln x)$. This is consistent with $x^0 = 1$.

In Figure 2 we show the how superposing plots for $\pm\gamma(\tau;n)$ produces a credible-looking yin-yang symbol. Here, $n = i/\pi$, however, it can be modified to alter the symbol to your taste. Note that for this curve the parameter τ varies over several orders magnitude and was better represented in log space. Figure 3 shows a comparison of this gamma pulse with the classic model. This traditional yin-yang is composed solely of circular segments; the inscribed "S-curve" has constant curvature and is not as aesthetically pleasing as the new model. The attached animations show the curve in Figure 2 being drawn and the evolution of the curve over the full range of positive imaginary *n*-values. Negative *n* merely produces the conjugate image (vertical flip).

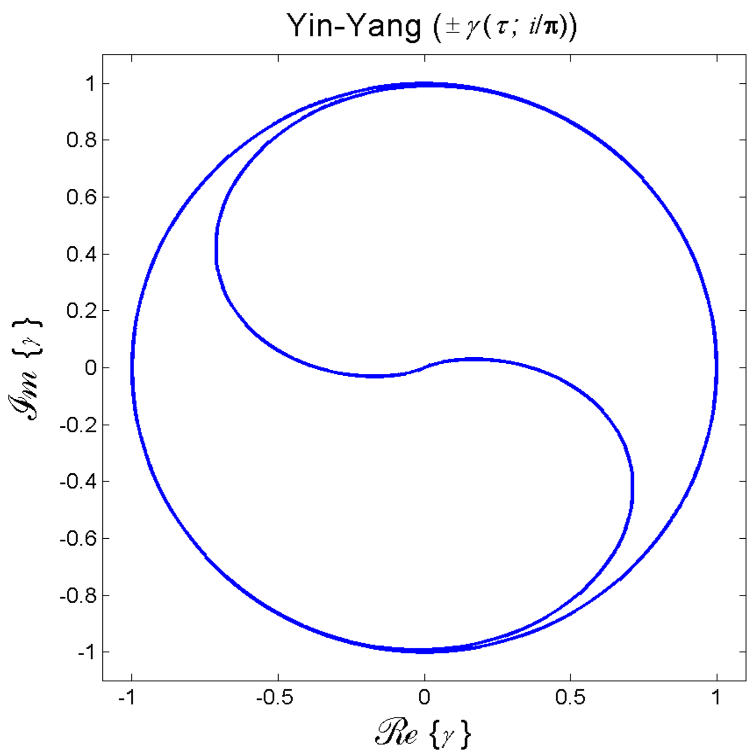

Figure 2: Yin-yang symbol, $\pm\gamma(\tau;i/\pi)$.

The effects of complex *n* are shown in Figure 4. They take on the form of nested globules and the number and position of the visible globules varies with the real and imaginary parts of *n*. Referring to Figure 4 and letting $n = N + iK$, a casual observation shows that the figure becomes increasingly complex (i.e., more and larger globules) with decreasing *N* or increasing *K*, and vice versa. The attached animation shows the nested globules as we zoom in an astonishing 43 orders of magnitude. This was limited only by our software. The true depth of the nesting is as yet unknown.

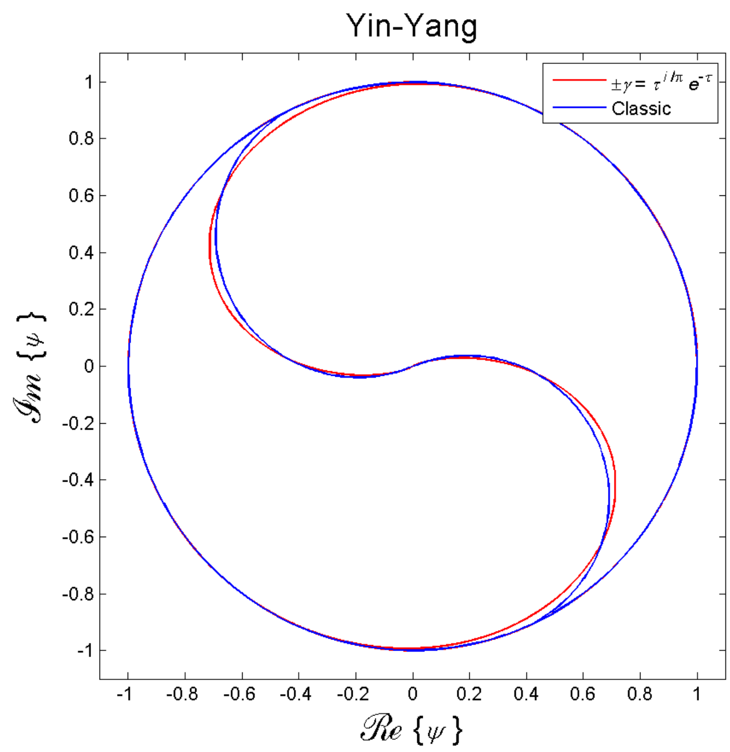

Figure 3: Yin-yang symbol, $\pm\gamma(\tau;i/\pi)$ and classic model.

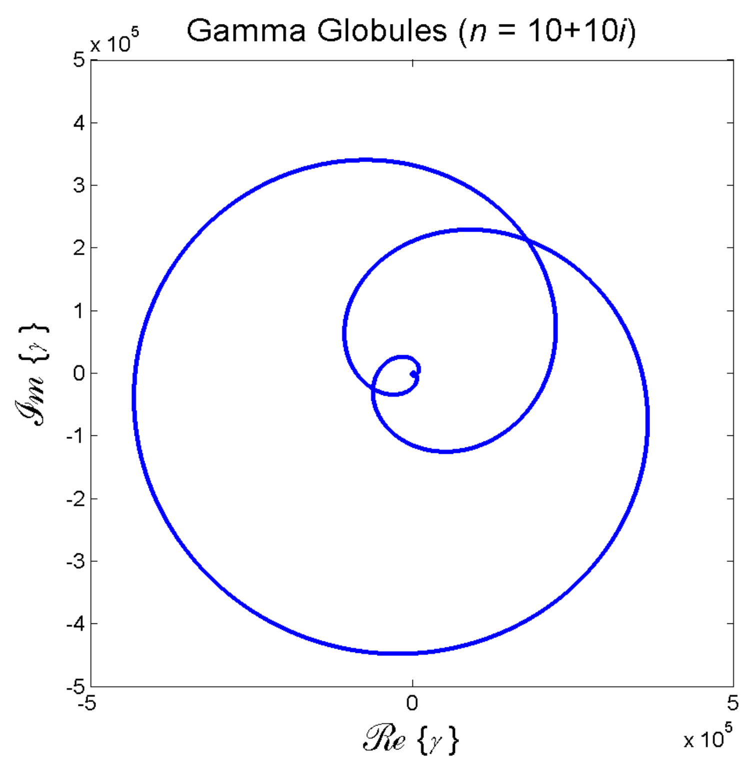

Figure 4: Gamma globules (*n* = 10+10*i*).

The sample Matlab code below should be sufficient to get you started.

```
p=inline('tau.^n.*exp(-tau)','tau','n');
tau=linspace(0,10,1e6+1)';
n=10+10i;
figure;plot(p(tau,n));axis equal
```

The specific Matlab code for the yin-yang is

```
p=inline('exp(n*log(tau)).*exp(-tau)','tau','n');
tau=logspace(-11,1,1e6+1);
n=i/pi;
pyy=p(tau,n);
q=[pyy;-flipud(pyy)];
figure;plot(q);axis(1.1*[-1 1 -1 1]);axis square
```

In summary, we have developed a new class of curves in the complex plane that includes limit cycle spirals, the yin-yang symbol, and the gamma globules.

An alternative take on the Yin-Yang curve

Banakh *et al*. ("Fermat's Spiral And The Line Between Yin And Yang," arXiv:0902.1556v2, 2009) take a different approach to the yin-yang curve. Their analysis is rather involved and beyond the scope of this paper. Let it suffice to say that they prove that Fermat's spiral is a unique yin-yang line in the class of smooth curves algebraic in polar coordinates.

Fermat's spiral in polar coordinates can be expressed as $r^2 = a\theta$. Without loss of generality, we can take the constant *a* to be unity and the entire yin-yang family of curves can be expressed in the complex plane as $z(\theta) = \pm\theta^{1/2}e^{i\theta}$. Figure 5 [after Banakh et al. (2009)] shows Fermat's spiral and some example bounding circles which define the yin-yang curves within. As the circles increase in radius, the yin-yang curve wraps around itself. The same effect is seen in the gamma pulse, albeit with changes in the pulse order, as demonstrated in Figure 6, except that here all the curves are bound by the circle of unit radius. The major difference between these two models is that the Fermat spiral crosses the bounding circle whereas the gamma pulse approaches it asymptotically. This is seen quite clearly in a comparison with the Fermat spiral bounded by the unit circle, as seen in Figure 7. The Fermat spiral exhibits kinks in the nose of the yin and yang while the gamma pulse is smooth throughout.

What we learn from Banakh *et al*. is to regard the yin-yang curves as a complete family that divides a disc into two congruent perfect sets in a specific way. They accomplish this intentionally for an algebraic polar equation and end up with Fermat's spiral. We accomplished a similar result inadvertently with a gamma pulse of imaginary order.

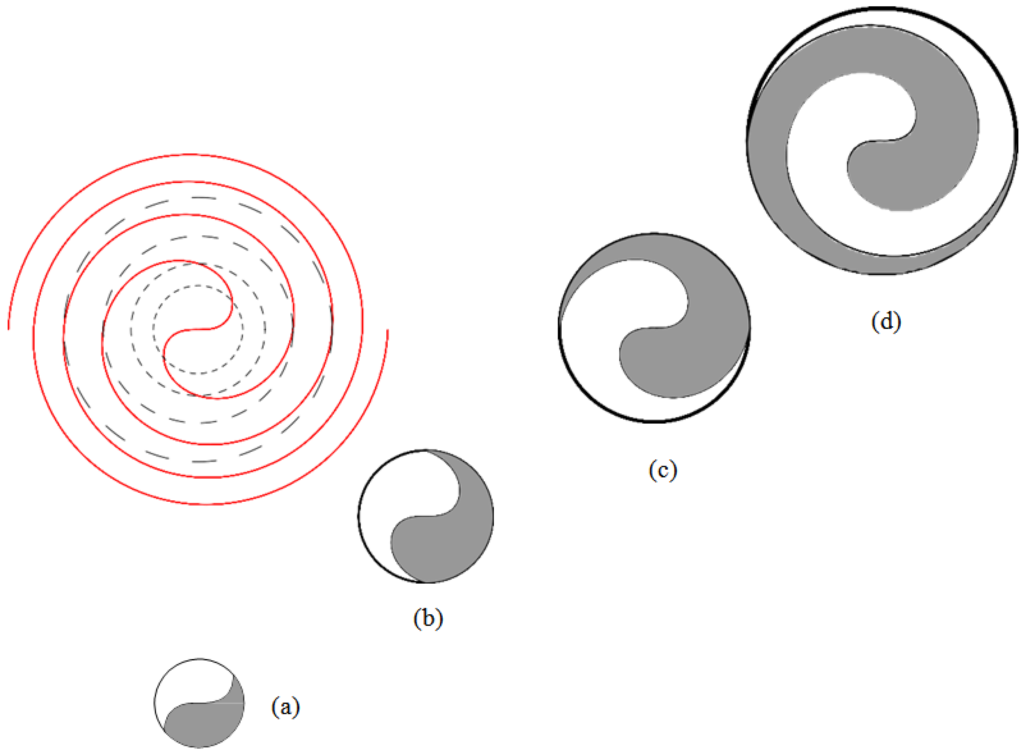

Figure 5: Fermat's spiral and yin-yang curves [after Banakh *et al*. (2009)].

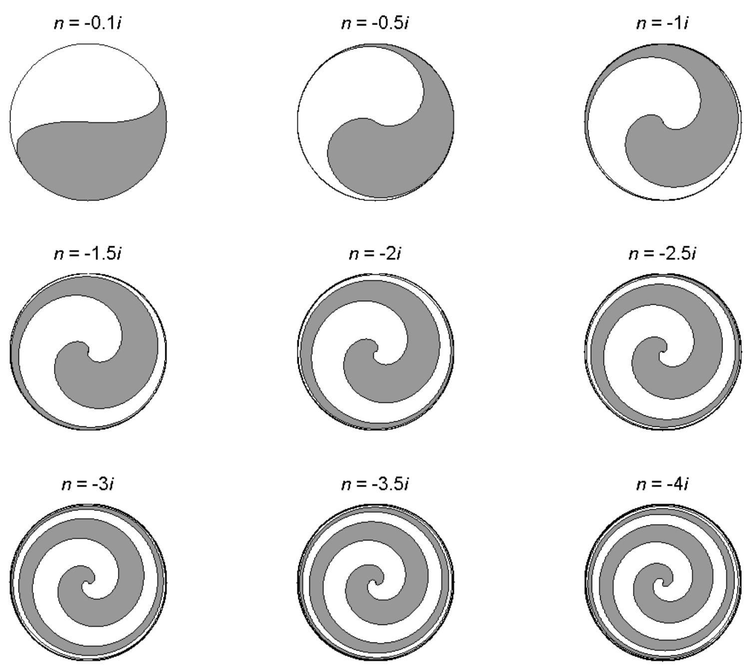

Figure 6: Example yin-yang curves from the gamma pulse with imaginary order *n*.

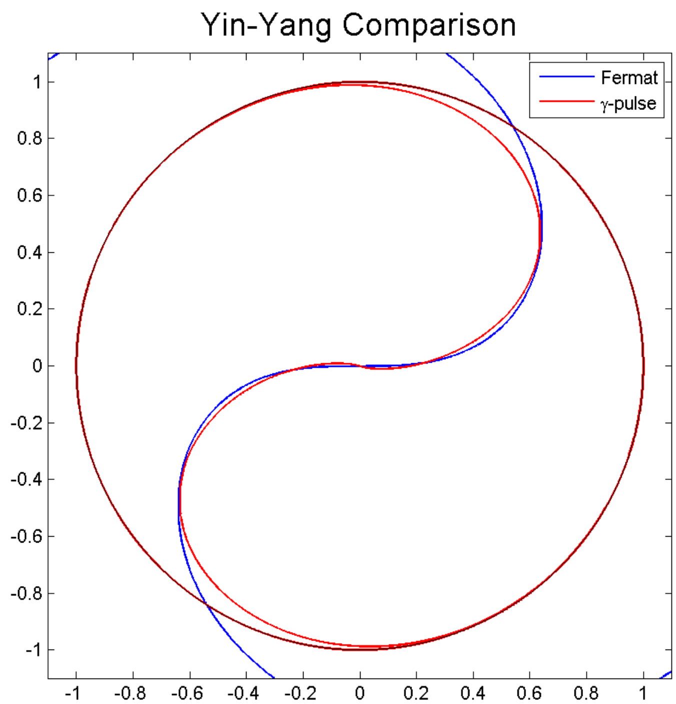

Figure 7: Comparison of yin-yang curves of Fermat's spiral (unit radius) and gamma pulse, $n = -i/\pi$ **.**

Physical pulses

In physical systems, a pulse can be adequately defined with two parameters: the rise time and the pulse width. These can be modeled with a gamma pulse of order *n* and characteristic frequency *k*. In physical space the pulse is given by

$$\begin{aligned} &\gamma(t;n) = k(kt)^n e^{-kt} u(t) \\ &\int_0^\infty \gamma(t;n)\,dt = \Gamma(n+1) \end{aligned} \tag{6}$$

The pulse appropriately has the dimensions of inverse time. In the analysis we shall use the dimensionless time $\tau = kt$.

In the present effort we show how to relate the pulse order and characteristic frequency to the rise time and the pulse width. Thus, $k = \Delta\tau/\Delta t$, where Δt is a user specified pulse width in physical space and $\Delta\tau$ is a dimensionless pulse width to be determined in this analysis. We shall, in fact, look at several criteria for the pulse width: rms pulse width, inflection points, Gaussian, and full-width-half-max (FWHM) or 3dB pulse width. The dimensionless pulse width will be seen to a function of the pulse order only.

Figure 8 shows a sampling of pulses of orders $n = 0.1 \rightarrow 1000$ for a millisecond pulse (in physical time). Note that these curves are normalized to unit area. The overlaid black lines are the asymptotic solutions for large pulse orders (see below).

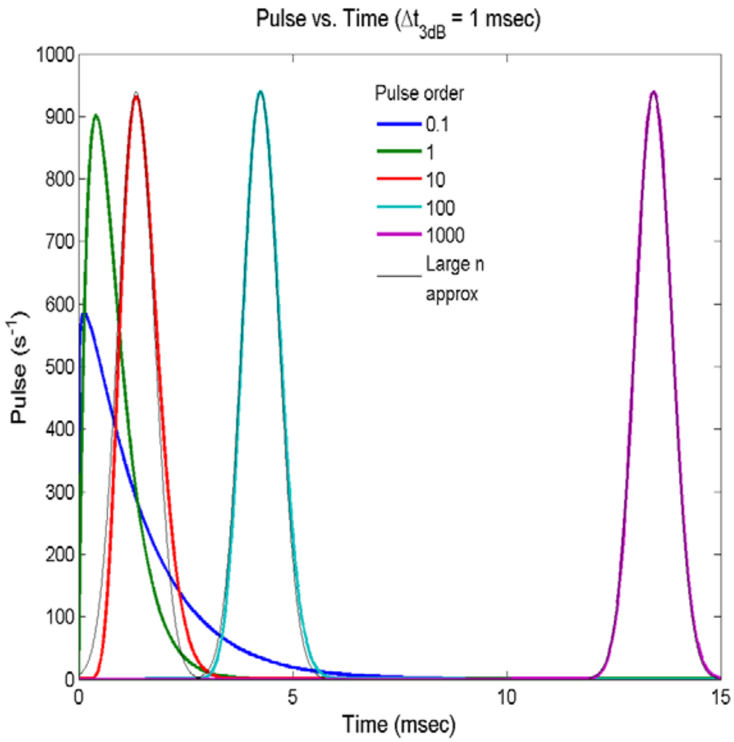

Figure 8: Gamma pulses of various orders.

We now examine some properties of the pulse in order to ascertain the pulse width in similarity space, $\Delta\tau$. The gamma pulse properties are summarized below:

(a) Time to maximum signal (i.e., the dimensionless rise time)

$$\left.\frac{\partial\gamma(\tau;n)}{\partial\tau}\right|_{\tau^*} = 0 \rightarrow \tau^* = n \tag{7}$$

(b) Inflection points (two for $n \geq 1$, but only one real inflection point for $n < 1$)

$$\left.\frac{\partial^2\gamma(\tau;n)}{\partial\tau^2}\right|_{\tau^{**}} = 0 \rightarrow \tau^{**} = n \pm \sqrt{n} \quad \& \quad \Delta\tau_{\text{inf}} = 2\sqrt{n} \quad (n \geq 1) \tag{8}$$

(c) Mean time

$$\bar{\tau} = \frac{\int_0^\infty \tau\,\gamma(\tau;n)\,d\tau}{\int_0^\infty \gamma(\tau;n)\,d\tau} = \frac{\Gamma(n+2)}{\Gamma(n+1)} = n+1 \tag{9}$$

(d) rms pulse width

$$\tau_{\text{rms}}^2 = \frac{\int_0^\infty (\tau-\bar{\tau})^2 \gamma(\tau;n)\,d\tau}{\int_0^\infty \gamma(\tau;n)\,d\tau} = \frac{\Gamma(n+1)\cdot\Gamma(n+3)-\Gamma^2(n+2)}{\Gamma^2(n+1)} = n+1 \tag{10}$$

(e) Asymptotic behavior (large *n*)

$$\gamma(\tau;n) \approx \frac{\Gamma(n+1)}{\sqrt{2\pi\cdot n}} e^{-\frac{(\tau-n)^2}{2n}} \quad \text{as } n\to\infty \tag{11}$$

and

$$\begin{gathered} \gamma(t;n) = \frac{\Gamma(n+1)}{\sigma\sqrt{2\pi}} e^{-(t-\mu)^2/2\sigma^2} \quad \text{as } n\to\infty \\ \mu = \sqrt{n}\cdot\sigma = n/k \\ \sigma = \Delta t_{\text{3dB}} \big/ 2\sqrt{2\ln 2} = \sqrt{n}\big/k \end{gathered} \tag{12}$$

(f) 3dB pulse width

$$\begin{aligned} \Delta\tau_{\text{3dB}} &\approx 2\sqrt{2\ln 2\cdot n} && n \gg 1 \\ \Delta\tau_{\text{3dB}} &\approx \sqrt{6\cdot n} && n = \mathcal{O}(1) \\ \Delta\tau_{\text{3dB}} &\approx \sqrt{(0.7)^2 + \left(2\sqrt{2\ln 2\cdot n}\right)^2} && \text{all } n \text{ (empirical)} \end{aligned} \tag{13}$$

Figure 8 shows the asymptotic solutions overlaid on the exact solutions for values of $n \geq 10$. The figure also emphasizes the fact that the magnitude of the area-normalized pulse approaches a constant value that is given by

$$\frac{\gamma(t^*;n)}{\Gamma(n+1)} = \frac{2}{\Delta t_{\text{3dB}}} \sqrt{\frac{\ln 2}{\pi}} \quad \text{as } n\to\infty \tag{14}$$

Furthermore, it follows from the Fourier transform, Eqs. (2) that

$$\psi(\tau;n) \approx i^n \Gamma(n+1) e^{-in\tau} e^{-\frac{\tau^2}{2n}} \quad \text{as } n\to\infty \tag{15}$$

That is, for large *n* the Cauchy pulse becomes sinusoidal with a Gaussian envelope.

Figure 9 shows a comparison of the exact 3dB pulse width compared with some approximations. The empirical value shown in Eq. (13) has an error of less than 1%. This result is virtually indistinguishable from the numerical solution at the scale of this figure.

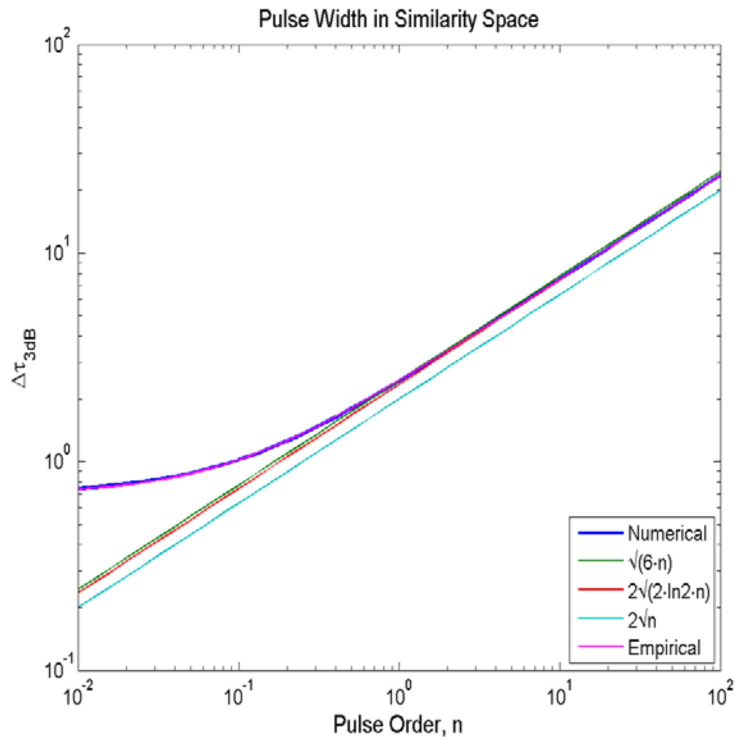

Figure 9: Pulse width in similarity space.

In summary, we have developed a model pulse for physical systems that gives the user control over the pulse width and the rise time, or in the case of large *n*, the delay time.

Please feel free to direct any inquiries to me at cye@att.net. And certainly inform me of your own discoveries. Thanks.